

Narrow-Band, Band-Pass Filters with Zig-Zag, Hairpin-Comb Resonators

George L. Matthaei

Superconductor Technologies Inc., Santa Barbara, CA 93111

Abstract “Hairpin-comb” filters have been previously shown to have special properties which are advantageous for the design of compact, narrow-band, band-pass microstrip filters. Herein a new “zig-zag” form of hairpin-comb filter is introduced which is shown to have additional important advantages for designing compact narrow-band filters. Examples with computed and measured results are presented.

I. INTRODUCTION AND GOALS

Currently there are numerous applications where microstrip, narrow-band filters are desired which are as of small size as possible. This is particularly true for wireless applications where high-temperature superconductor (HTS) technology is being used in order to obtain filters of small size with high resonator Q's. The filters required are often quite complex with perhaps 12 or more resonators along with some cross couplings. Yet the wafers available for HTS filters usually have a maximum size of only two or three inches. Hence, means for achieving filters as small as possible while preserving high-quality performance are very desirable. Therefore, the goals of this work are to achieve:

- 1) Very small, compact resonators.
- 2) Weak couplings between resonators (as are required for narrow-band filters) while maintaining relatively small spacings between resonators. This is important because in the case of many microstrip resonator structures, in order to achieve narrow bandwidth, quite large spacings between resonators are required.
- 3) Very low parasitic coupling to resonators beyond nearest neighbor resonators so that unwanted parasitic couplings can be ignored in the design process. This is important so that the field solver used in the design process will only have to analyze pairs of resonators at a time.

II. PROPERTIES OF HAIRPIN-COMB FILTER STRUCTURES

The filters discussed herein are closely related to the “hairpin-comb” filter configuration shown in Fig. 1(b). As is discussed in [1], [2], this type of filter structure has properties which are quite useful for narrow-band filters. Figure 1(a) shows what is commonly referred to as a “hairpin-line” filter. (See [3] for example.) Note that in this structure the orientations of the hairpin resonators alternate. This is done because it causes the electric and magnetic couplings to tend to add, thus resulting in maximum coupling for a given spacing between resonators. This is desirable for most applications but is very poor for the case of narrow band filters since then very large spacings between resonators will be required. In the case of the hairpin-comb configuration in Fig. 1(b) the resonators all have the same orientation which causes the electric and magnetic couplings to tend to cancel. Using this structure, narrow-band microstrip filters can be realized with much smaller spacings between the resonators. Hence, this principle is incorporated in the present work.

A subtle but important phenomena that occurs in microstrip hairpin comb structures is that a resonance effect occurs in the vicinity of the coupling region between resonators, and this creates a pole of attenuation adjacent to the passband. If the hairpin-comb structure is in a homogeneous dielectric this pole will occur above the passband. However, in the case of conventional microstrip using a dielectric substrate, the even- and odd-mode wave velocities for pairs of coupled lines are different, and it turns out that the pole of attenuation typically occurs *below* the passband. However, the position of this pole of attenuation can be controlled to some extent by the addition of capacitive coupling between the open ends of adjacent resonators as is shown in Fig. 2. It turns out that as small amounts of capacitance C are *added* as shown in Fig. 2, the pole of attenuation moves *upwards* in frequency and causes the passband to be further narrowed [1], [2]. At some point the pole will move into the passband and kill the passband completely. Adding still more

capacitance C will cause the pole to move up above the passband. This control of the pole position is a potentially useful feature of hairpin-comb structures. In the case of the zig-zag hairpin-comb structures about to be discussed there are more degrees of freedom present, and the pole position for the case of $C = 0$ can be on either side of the passband depending on the design of the zig-zag structure.

III USE OF ZIG-ZAG HAIRPIN-COMB RESONATORS

The use of hairpin-comb filter structures is seen to be helpful in obtaining relatively small filters with resonators that lend themselves to quite high unloaded Q 's. However, for applications where large numbers of resonators must be used on substrates of very limited size, or for filters on such substrates with a modest number of resonators but with their pass band at relatively low frequencies (say, in the one hundred MHz range), even more compact structures are needed. In order to meet this need we have investigated hairpin-comb structures in which the hairpin-line structures are zig-zaged (or meandered) in order to reduce the size of the hairpin structure while at the same time presenting very limited coupling to adjacent structures.

Figure 3 shows a two-resonator, trial, HTS, microstrip zig-zag hairpin-comb filter structure that we have analyzed using Sonnet [5], and fabricated and tested. The center frequency of the filter is roughly 2 GHz, and it uses a 0.508-mm-thick MgO ($\epsilon_r = 9.7$) substrate along with TBCCO superconductor. The resonators are 3.49 mm wide and 4.8 mm high with a space of 0.45 mm between resonators. The resonators could have been proportioned differently if that was desirable. Note that most of the line sections in the resonators are oriented horizontally. Hence, the segments of this sort in one resonator couple very little to the corresponding ones in the other resonator. Most of the magnetic coupling between resonators comes from the short vertical sections adjacent to the gap between the resonators. Similarly, most of the electric coupling also comes from the vicinity of the vertical sections adjacent to the coupling gap. The degree of coupling between resonators is strongly influenced by the length chosen for these vertical sections as well as by the spacing between the resonators. In this trial design we used inductive-tap couplings at the input and output of the filter, though we could have, instead, used series-capacitance coupling at the upper left and upper right of the filter for coupling to the terminations.

The dashed lines in Fig. 4 show the responses for this structure computed using Sonnet [5], while the solid lines

shows the response measured at 77 K.. The measured bandwidth at the 3-dB level is 26 MHz which compares well with the computed 3-dB bandwidth of 26.7 MHz. The measured passband ripple is somewhat larger than the computed ripple. We believe this was at least largely due to the fact that the metal mounting structures on the available dielectric tuners were too large to permit placing the centers of the tuners as close together as were the centerlines of the resonators. This meant that the tuners affected the two sides of the resonators unequally. It can be shown that such asymmetry in loading the sides of a tapped hairpin resonator throws off the effective electric position of the tap so as to increase the Q_e . Larger Q_e 's result in larger passband ripples. The measured passband center is around 13.9 MHz higher than was computed. In the Sonnet calculations a 0.025 mm square cell size was used, and it was of interest to see what affect reducing the cell size would have on the computed results. Using a somewhat simplified but closely related filter structure with about the same center frequency and bandwidth, responses were computed with 0.025 square cells and with 0.0125 square cells. The computed bandwidth was virtually the same for both cases but the smaller cell size gave a center frequency that was about 8.2 MHz higher. Thus it appears likely that more than half of the difference between the computed and measured center frequencies in Fig. 4 was probably due to the finite cell size in the calculations. Preliminary measurements of the resonator unloaded Q 's suggests Q 's in excess of 39,000.

In Fig. 4 the attenuation on the high side is seen to be unusually sharp due to a pole of attenuation at 2.058 GHz, while the attenuation is somewhat weak on the low side of the pass band. Interestingly enough, tap connections as shown in Fig. 3 can in be used to enhance the attenuation by creating additional poles of attenuation on both sides of the passband. These result from quarter-wave resonances in the two sides of the resonator which short out the tap at frequencies somewhat above and below the resonator center frequency. Though we have seen this effect work well in other examples it was lost in this example, possibly due to stray coupling between the input and output lines. In the four-resonator example about to be discussed the input and output lines are further apart and these poles of attenuation are realized.

Figure 5 shows the aforementioned four-resonator trial filter structure. In order to expedite the design of an initial, trial, 4-resonator structure we decided to use the same couplings to the terminations as used in Fig. 3, and the same 0.450-mm spacings between resonators 1 and 2 and between resonators 3 and 4 as was used between the resonators in Fig. 3. Then the spacing between resonators

2 and 3 was adjusted to yield a roughly equal-ripple response (i.e., 0.500 mm). The structure in Fig. 4 is too complex to analyze with Sonnet using the computing power presently available. Hence, instead, we worked with Sonnet to compute a value Q_e for the external Q of the end resonators and for the coupling coefficients between pairs of resonators. This was accomplished using modeled singly loaded test resonators, and also coupled pairs of test resonators. The principles used were similar to those discussed in Ref. [4]. For a given Q_e and coupling coefficients between resonators the approximate expected frequency response was easily computed using a simplified filter model having half-wavelength, open-circuited shunt-stub resonators with frequency-independent inverters in between.

One of the things that we wanted to confirm with the example in Fig. 5 was that coupling beyond nearest neighbor resonators can be ignored and still obtain accurate designs. To at least get some feel for the answer to this question we tried computing the coupling between resonators 1 and 3 in Fig. 5 with resonators 2 and 4 removed. The computed coupling coefficient was $k_{13} = 0.0001696$, as compared to $k_{12} = 0.009483$ for coupling between resonators 1 and 2. We see that $k_{13}/k_{12} \sim 1/56$. Thus k_{13} appears to be sufficiently small compared to k_{12} so that it can probably be neglected. Of course, with resonator 2 in place the value for k_{13} may be somewhat different. Similar calculations between resonators 1 and 4 with 2 and 3 removed give $k_{14}/k_{12} \sim 1/285$.

The solid lines in Fig. 6 show the measured response for the HTS trial filter in Fig. 5, while the dashed lines show the response computed from the aforementioned simplified model using a Q_e and coupling coefficient values obtained using Sonnet. For easy comparison of responses the computed response was centered on the middle of the measured response. As was also true for the two-resonator case in Fig. 3 the measured pass band ripples are larger than are the computed ripples. Again, we believe this was, at least, largely due to asymmetric positioning of the available dielectric tuners that had metal mounts that were a little too large. In Fig. 6 the measured 3-dB bandwidth is 27.27 MHz while the 3-dB bandwidth computed from the simplified model was 28.18 MHz. Note that the measured response exhibits poles on both sides of the pass band for reasons previously mentioned. The slightly smaller measured 3-dB bandwidth as compared to the computed response is due, at least in part, to the fact that

the computed response does not have adjacent poles (which would tend to narrow the pass band). Thus it appears that the interior coupling coefficients were realized with very good accuracy, and there is no evidence of any measurable effect due to stray coupling beyond nearest neighbor resonators.

IV. CONCLUSIONS

It is seen that the use of microstrip zig-zag hairpin-comb filter structures can give unusually compact filters for applications where very narrow bandwidths are required. The structures provide a relatively large degree of design flexibility in proportioning the physical structure and in placing poles beside the pass band.

ACKNOWLEDGEMENT

The research described in this paper was supported in part by DARPA under Contract MDA972-00-C-0010. The author wishes to thank Kurt Raihn and Balam Willemsen of STI for their kind assistance in the preparation of this paper.

REFERENCES

- [1] G. L. Matthaei, N. O. Fenzi, R. J. Forse, and S. M. Rohlfing, "Hairpin-comb filters for HTS and other narrow-band applications," *IEEE Trans. Microwave Theory and Tech.*, vol. 45, no. 8, pp. 1226-1231, August 1997.
- [2] G. L. Matthaei, "Microwave hairpin-comb filters for narrow-band applications," US Patent No. 6,130,189, Oct. 10, 2000.
- [3] E. G. Cristal and S. Frankel, "Hairpin-line and hybrid hairpin-line half-wave parallel-coupled-line filters," *IEEE Trans. Microwave Theory and Tech.*, vol. 20, no. 11, pp. 719-728, November 1972
- [4] G. L. Matthaei, L. Young, and E. M. T. Jones, *Microwave Filters, Impedance-Matching Networks, and Coupling Structures*, Norwood, MA: Artech House, 1980, Secs. 11.02 and 11.04.
- [5] Sonnet Software, Inc., Liverpool, NY 13088.

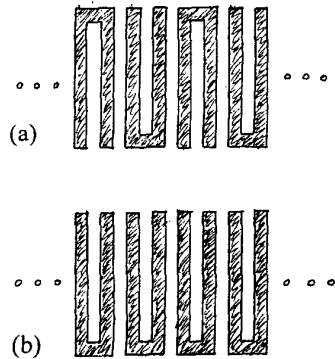


Fig. 1 At (a) is shown a conventional "hairpin-line" filter structure, while at (b) is shown a "hairpin-comb" filter structure

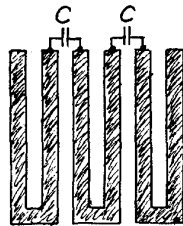


Fig. 2 A hairpin-comb structure with capacitances C added between the resonators.

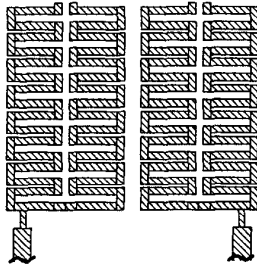


Fig. 3 A trial, two-resonator "zig-zag hairpin comb" filter.

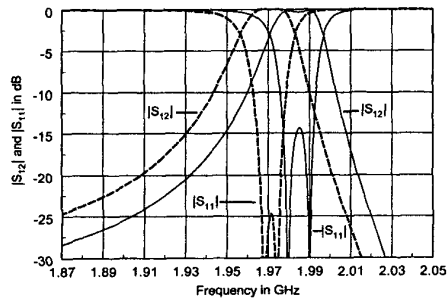


Fig. 4 The solid lines show the measured responses for the filter in Fig. 3 while the dashed lines show the responses computed using Sonnet [5].

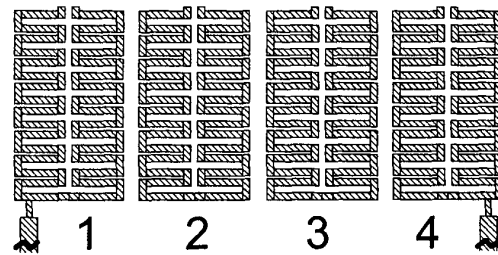


Fig. 5 A trial 4-resonator filter structure

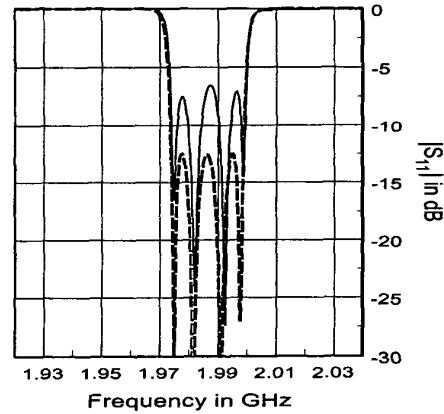
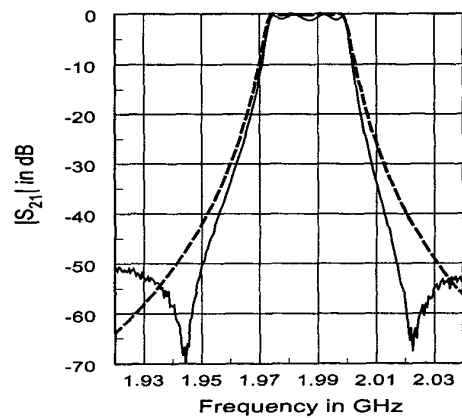


Fig. 6 The solid lines show the measured results for the filter in Fig. 5, while the dashed lines show results computed from a simple model along with coupling coefficients and external Q 's obtained using Sonnet [5].